IMPLEMENTATION ON PALM PRINT BY GLOBAL FEATURES

DHANUSHIA BEULAH.T Student,
Dr.T. Arumuga Maria Devi BE,M.,Tech.,Ph.D.,
AP-CITE,
Manonmaniam Sundaranar University,
Abishekapatti, Tirunelveli.

Abstract: Three-dimensional (3-D) palm print has proved to be a significant biometrics for personal authentication. Three- dimensional palm prints are harder to counterfeit than 2-D palm prints and more robust to variations in illumination and serious scrabbling on the palm surface. Previous work on 3-D palm-print recognition has concentrated on local features such as texture and lines. In this paper, I propose three novel global features of 3-D palm prints which describe shape information and can be used for coarse matching and indexing to improve the efficiency of palm-print recognition, particularly in very large databases. The three proposed shape features are maximum depth of palm center, horizontal cross-sectional area of different levels, and radial line length from the centroid to the boundary of 3-D palm-print horizontal cross section of different levels. I use orthogonal linear discriminate analysis to reduce their dimensionality. I then adopt two schemes: 1) coarse-level matching and 2) ranking support vector machine to improve the efficiency of palm-print recognition. I conducted a series of 3-D palm-print recognition experiments using an established 3-D palm-print database, and the results demonstrate that the proposed method can greatly reduce penetration rates.

***Index Terms*—Global features, orthogonal linear discriminant analysis (LDA) (OLDA), palm-print indexing, ranking support vector machine (SVM) (RSVM), 3-D palm-print identification.**

I. INTRODUCTION

PALM PRINT recognition has now been a topic of research for over 10 years. Like other biometrics, palm prints demonstrate the properties required for personal authentication, universality, uniqueness, performance, collectability, and acceptability [1]. Furthermore, palm prints have some advantages over other biometrics. Palm prints are larger than fingerprints and therefore more robust to scars and dirt. Palm print images are cheaper to collect and more acceptable than iris. Palm prints can distinguish between individuals more accurately than face and can also identify monozygotic twins [2].

Traditionally, palm-print recognition has made use of either high- or low-resolution 2-D palm-print images. High-resolution images are suitable for forensic applications [3], while low-resolution images are suitable for civil and commercial applications [4]. Most current research uses low-resolution palm print recognition and is either texture based or line based. The texture-based methods include Palm Code [4], Competitive Code [5], and Ordinal Code [6]. These methods use a group of filters to enhance and extract the phase or directional features which can represent the texture of the palm print. Line based methods use line or edge detectors to explicitly extract line information from the palm print that is then used for matching. The representative methods include derivative-of-Gaussian-based line extraction [7] and modified-finite-Radon transform-based line extraction [8].

In recent years, 3-D techniques have been applied to biometric authentication, such as 3-D face [9], [10] and 3-D ear recognition [11]. Most recently, a structured-light-imaging [12], [13]3-D palm-print system [14], [15] was developed that captures the depth information of a palm print. This information is then used to calculate the mean and the Gaussian curvatures for use in 3-D palm-print matching and recognition. For fingerprint, according to the global ridge structure and singularities, it can be classified into five classes: arch, tented arch, left loop, right loop, and whorl [16]. Reference [17] classified the palm print into six classes according to the palm print principal lines. Besides the exclusive classification technique, the continuous classification technique is also widely used for indexing the database for personal identification [18].

In this paper, I propose extracting three novel global features from a 3-D palm-print image: maximum depth (MD) at the center of the palm, horizontal cross-sectional area (HCA)at different levels of the palm; and radial line length (RLL)measured from the centroid to the boundary of the 3-D palm print. These features are then used to describe and classify the shape of the 3-D palm print using continuous classification. This involves first reducing the dimensionality of the features by treating these features as a column vector and applying orthogonal linear discriminant analysis (LDA) (OLDA) [19].
I then improve the efficiency of palm-print recognition by indexing the database using coarse-level matching and ranking support vector machine (SVM) (RSVM) [20].

The rest of this paper is organized as follows. Section II describes how I define a region of interest (ROI) for the 3-D palm print image and then extract our three proposed global features. Section III describes how global features can be used in classification in order to speed up identification. Section IV gives the perimental results, and Section V concludes this paper.

ISSN: 2278 – 1323

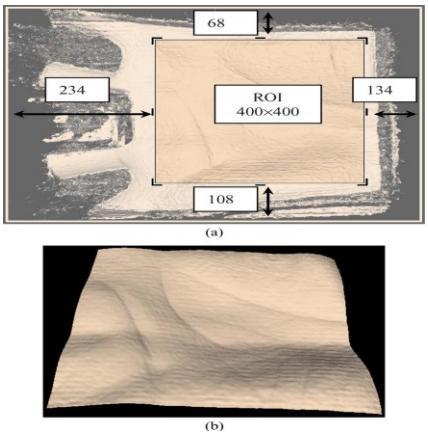

Figure. 1. ROI extraction of 3-D palm print. (a) Location of the ROI in the palm-print image. (b) Extracted 3-D ROI.

II. GLOBAL FEATURES: DEFINITIONS AND EXTRACTION

The following describes our procedure by first extracting a region of interest from the 3D palm print, and from each palm print extract our proposed three global features.

A. ROI

Our definition and extraction procedure makes use of a 3-D palm-print image containing 768 × 576 points captured using a structured-light-imaging-based 3-D palm-print acquisition device [14]. First, I remove redundant and noisy boundary regions using a very simple ROI extraction process (Fig. 1).I segment a 400 × 400 point square that is 68, 108, 234, and134 points from the top, bottom, left, and right boundaries of the 3-D palm-print image, respectively, as shown in Fig. 1(a).Fig. 1(b) shows the extracted ROI. After down sampling the 3-D ROI to 200 × 200 points, I store it in a 200 by 200matrix, {dij |i = 1, 2, . . . , 200; j = 1, 2, . . . , 200}, where dij is the depth value of the ith row and jth column point of the 3-D ROI.

Our proposed 3-D palm-print ROI extraction approach is much simpler than the one reported in [4], and the extracted shape features are not sensitive to translation and rotation, which is why I can use such a coarse ROI extraction. As the shape feature is a form of global feature, I extract as large a ROI as possible. Of course, such a large ROI may contain noisy data, so I use a mask to remove the noisy data according to the gradient of the 3-D data. If the gradient of the point, which is defined as

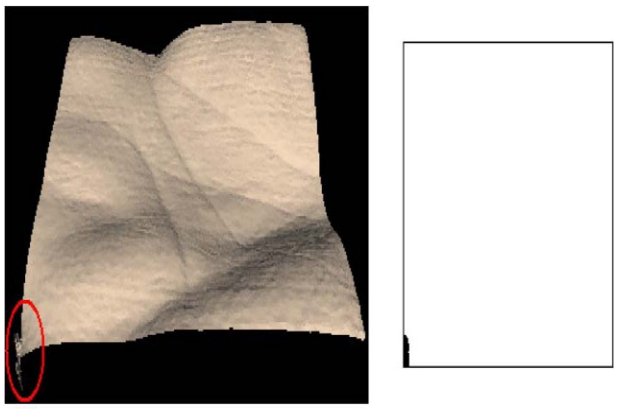

(a) (b)

$|\nabla d| = \sqrt{(\partial d/\partial x)2 + (\partial d/\partial y)2}$, is larger than a given threshold, the point is regarded as noisy data. Fig. 2 shows a 3-D ROI which contains noisy data and its corresponding mask. I use a 200 by 200 matrix, {mij |i = 1, 2, . . . , 200; j = 1, 2, . . . , 200}, to represent the mask, where mij = 0 is noisy data and mij = 1 is for other data.

B. Three Global Features

Using the ROI obtained from the original 3-D palm print data, I extract three kinds of features to describe the shape of the 3-D palm print: MD of palm center, the HCA of different levels, and the RLL from the centroid to the boundary of 3-Dpalm-print horizontal cross section of different levels.

1) MD: MD means the maximum depth value of the 3-D palm from a reference plane. The reference plane is decided using a rectangle as shown in the left of Fig. 3(a). The depth of the reference plane dr is the mean depth of the points contained by this rectangle

Where dij is the depth value of the ith row and jth column point of the 3-D ROI, mij is the corresponding mask value, and Rs,Re, Cs, and Ce denote the start row, end row, start column, and end column, respectively. The parameters Rs = 65, Re =136, Cs = 6, and Ce = 35 Ire set by experience. The reason I choose this region is that, in the 3-D ROI, it appears to be relatively flat.

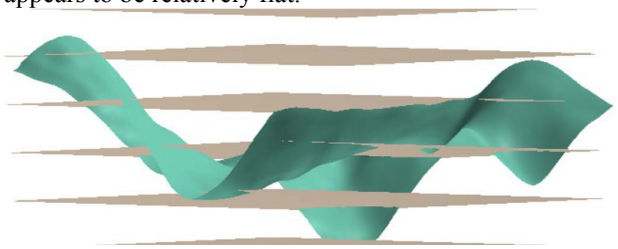

Figure. 4. Illustration of the 3-D ROI crossed by horizontal planes.

ISSN: 2278 – 1323

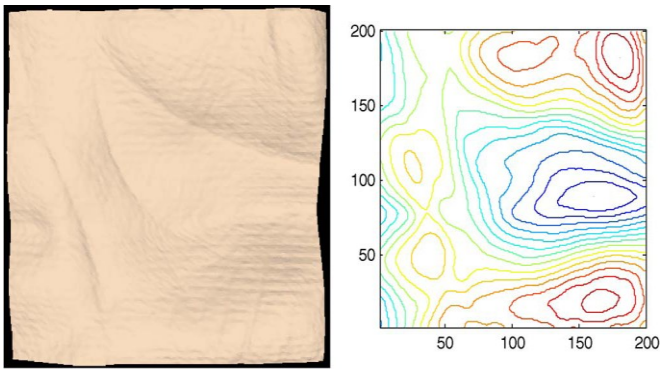

(a) (b)

Figure. 5. (a) Three-dimensional ROI. (b) Its corresponding contour cutting by the equidistant horizontal planes.

After getting the depth of the reference plane, I find the MD dmax in a region denoted by the right rectangle in Fig. 3(a) which starts at the 41st row and extends to the 160th row and from the 65th column to the 190th column. The MD can then be calculated easily by (2) as shown in Fig. 3(b)

$$MD = d\max - dr. \quad (2)$$

2) HCA: To describe the shape of the 3-D palm print, I use a group of equidistant horizontal planes to cut the 3-D ROI as shown in Fig. 4. Fig. 5 shows a 3-D ROI and its contour cut by the equidistant horizontal planes. To render the shape clearly, Fig. 5(a) only shows the 3-D ROI image and hides the equidistant horizontal planes. In Fig. 5(b), the blue curves denote deeper levels, the red curves denote higher levels, and the remaining curves are medium levels. The HCA is defined as the area enclosed by the level curve. From Fig. 5(b), I can see that most of the deeper level curves are enclosed and the areas are simply connected. These are more stable in response to noise or transformation. To get a stable HCA, I take into

$$d_w = \frac{1}{\sum_{i=R_s}^{R_e}\sum_{j=C_s}^{C_e} m_{ij}} \sum_{i=R_s}^{R_e}\sum_{j=C_s}^{C_e}(d_{ij}\cdot m_{ij}) \quad (1)$$

consideration only the levels from the deepest point to the reference plane, defined in Section III-A. Suppose I divide this region into N levels.

Every level Gk, k = 1, 2, . . .,N, is described with a 200 × 200 matrix and calculated by

$$G_{ij}^k = \begin{cases} 1, & \text{if } d_{ij} > h\cdot(N-k+1)/N \\ 0, & \text{otherwise} \end{cases}$$
$$k = 1, 2, \ldots, N;\ i = 1, 2, \ldots, 200;\ j = 1, 2, \ldots, 200 \quad (3)$$

Where dij is the depth value of the ith row and jth column point of the 3-D ROI and h is the palm print depth defined by (2).To make it more stable, I constrain every level growing from its previous level except the first level. That is,

$$Lk = Gk \cap (Lk-1 \oplus \Theta k-1),\quad k = 2,\ 3,\ \ldots,\ N;\ L1 = G1 \quad (4)$$

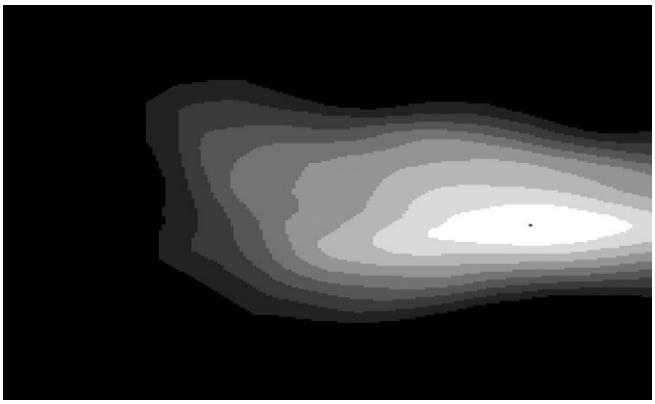

Figure. 6. Example of all the levels stacked together when $N = 8$.

where "∩" denotes logical AND, ⊕ denotes a morphological dilation operation, and Ok is a disk morphological structuring element whose size can be calculated by 35 − 3 × k (this is suitable for N = 8 by experience).Fig. 6 shows an example of all the levels stacked together. Fig. 7 shows each of the levels separately. After getting the cross-sectional levels Lk, k = 1, 2, . . .,N, the HCA Ak, k = 1, 2, . . . , N, can be easily calculated by

3) RLL: The HCA is only a coarse description of the cross section. To identify samples which have a similar cross sectional area but a different contour, I propose the RLL feature which describes the shape of the contour. First, I calculate the centroid of the first level L1; thereafter, I treat it as the centroid of all levels. Then, from the centroid, I draw M radial lines which intersect with the contour of every level. The distance between the intersection and the centroid is defined as the RLL. The radial lines are distributed at equal angles. I record these radial lines from the inner layers to the outer layers starting with the horizontal direction by an M× N dimensional vector Ri, i = 1, 2, . . . , M × N, where M is the number of radial lines and N is the number of cross sections. Fig. 8 shows some examples of radial lines and their cross sections. I can see that the RLL better represents the contour as the number of radial lines increases.

The aforementioned three global features are mainly determined by the central region of the palm. This region is certainly contained by the ROI described in Section II-A which makes these features insensitive to translation and rotation. Although the RLL feature can be affected by rotation as the contours change smoothly, if the rotation is small, then the variation of the RLL feature will

ISSN: 2278 – 1323

also be small. There are some restricting pegs on the capture device which can guide the user to put his/her hand on the proper place as described in[14]. Furthermore, I assume that the user is cooperative when collecting data as I aim at civil rather than law enforcement applications.

$$A^{lk} = \sum_{i=1}^{200} \sum_{j=1}^{200} L_{ij}^{lk}. \qquad (5)$$

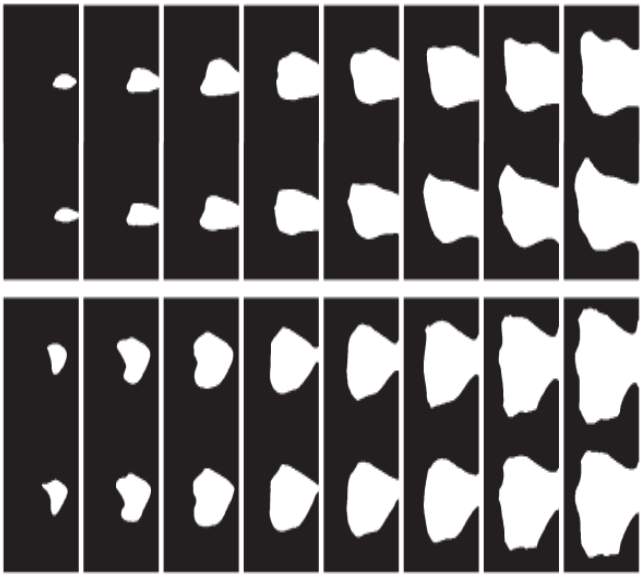

Figure. 7. Cross-sectional area feature (the top two rows are extracted from two samples collected from one palm, and the bottom two rows are extracted from two samples from another palm).

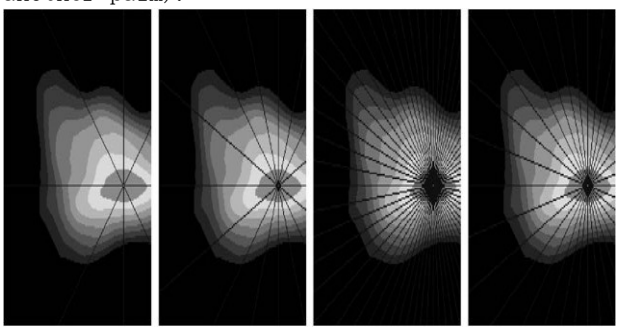

Figure. 8. Radial line starting from the centroid (from left to right: M = 8, 16,32, and 64, respectively).

III. CLASSIFICATION WITH GLOBAL FEATURES

The classification of biometrics speeds up the identification process by reducing the number of comparisons that must be made. There are two kinds of classification techniques exclusive classification and continuous classification. Both fingerprint[16] and palm-print classifications [17] make use of exclusive classification. The main problem of this technique is that it uses only a small number of classes and the samples are unevenly distributed between them, with more than 90%of the samples being in just two or three classes. A further problem with exclusive classification is that, when classification is performed automatically, it is necessary to handle errors and rejected samples gracefully, which is a hard problem in practice. In contrast, for continuous classification, samples are not partitioned into disjoint classes but rather associated with numerical vectors which represent features of the samples. These feature vectors are created through a similarity-preserving transformation. so that similar samples are mapped into close points in the multidimensional space [21]. In this paper, I adopt the continuous classification technique. As the global features combining MD, HCA, and RLL are high dimensional, I reduce the dimensions using the LDA method. I then improve the efficiency of palm-print recognition by applying coarse level matching and RSVM to the low-dimensional vectors.

A. Dimension Reduction Using OLDA

LDA is a state-of-the-art dimensionality reduction technique widely used in classification problems. The objective is to find the optimal projection which simultaneously minimizes the within-class distance and maximizes the between-class distance, thus achieving maximum discrimination (here, the "class" is used to denote the identity of the subjects, e.g., the samples collected from one palm are regarded as one class).However, the traditional LDA requires the within-class scatter matrix to be nonsingular, which means that the sample size should be large enough compared with its dimension, but is not always possible. In this paper, I therefore adopt the OLDA proposed in [19], where the vectors of the optimal projection are calculated using the training database and the optimal projecting vectors are orthogonal to each other. Suppose that the 3-D ROI has

$$(d_i, d_j) \in f_{\vec{w}}(q) \Leftrightarrow \vec{w}\phi(q, d_i) > \vec{w}\phi(q, d_j) \qquad (18)$$

been divided to N levels and that M radial lines are used to represent the level contours. I can list the global features as a column vector, F ={MD,A1,A2, . . . , AN,R1,R2, . . . , RN×M}, with 1+N+N ×M rows.

$$H_t \xrightarrow{\text{Reduced SVD}} U_w \Sigma_w V_w^T. \qquad (10)$$

Given a training database which has n samples and k classes as X = [X1,X2, . . . , Xk], where Xi ∈ _(1+N+N×M)×ni ,i = 1, 2, . . . , k, and n =_ki=1 ni, adopting OLDA [19], the optimal projection W can be calculated as follows. First, the within-class scatter matrix Sw, the between-class

ISSN: 2278 – 1323

scatter matrix Sb, and total scatter matrix St can be expressed as

$$S_w = H_w H_w^T, \quad S_b = H_b H_b^T, \quad S_t = H_t H_t^T \qquad (6)$$

Figure. 9. Flowchart of registration and recognition with coarse-level matching scheme.

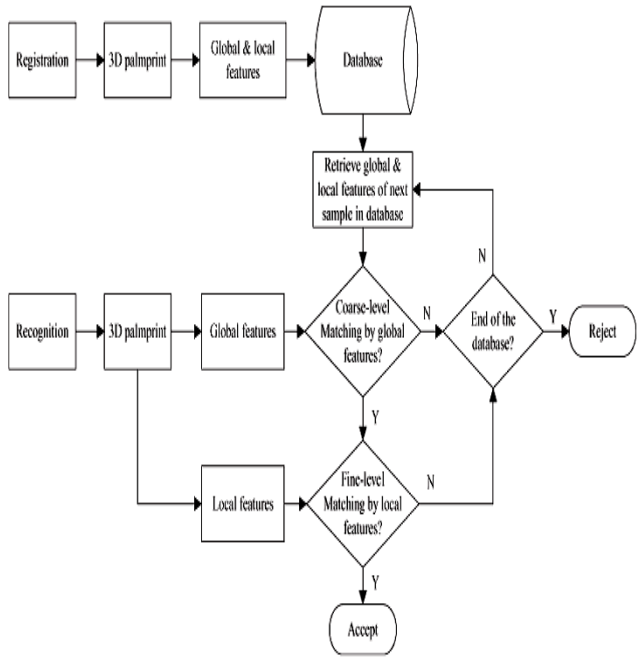

where $\widetilde{F} = \{f_1, f_2, \ldots, f_\Gamma\}$ is a Γ-dimensional vector with $\Gamma < 1 + N + N \times M$.

Coarse-Level Matching

$$\Delta = \|\widetilde{F}^1 - \widetilde{F}^2\|_2 = \sum_{i=1}^{\Gamma} \left(f_i^1 - f_i^2\right)^2. \qquad (16)$$

In 3-D palm-print identification, I can use the Γ-dimensional global features to carry out coarse-level matching as shown in Fig. 9. If the testing sample passes coarse-level matching, it undergoes fine-level matching using3-D palm-print local features. If it does not pass, it moves on to the next sample in the database and so on until it has accessed the last sample in the database. From (16), I can see that

coarse-level matching requires only Γ times of addition and multiplication which is much faster than fine-level matching using local features. Equation (17) gives the fine-level matching by mean curvature image (MCI) feature [14]

where symbol "∩" represents the logical AND operation and Zd and Zt are the two binaries MCI features. To deal with the translation problem of ROI when calculating the matching score by (17), I will shift two, four, six, and eight

$$Y = \frac{2\sum_{i=1}^{n}\sum_{j=1}^{m} Z_d(i,j) \cap Z_t(i,j)}{\sum_{i=1}^{n}\sum_{j=1}^{m} Z_d(i,j) + \sum_{i=1}^{n}\sum_{j=1}^{m} Z_t(i,j)} \qquad (17)$$

pixels of the test image along eight directions: right, left, up, down, left–up, left–down, right–up, and right–down, respectively. Adding then on shift one, I will have 8 × 4 + 1 = 33 matching scores, and the maximum one is selected. Suppose the size of the MCI feature is 128 × 128, i.e., m = 128 and n = 128, from (16) and(17), I can see that coarse-level matching is much faster than fine-level matching.

B. RSVM

Coarse-level matching scheme is a simple and easy way to reduce retrieval times. It is more useful for palm-print recognition if I can rank the candidate samples in the database in descending order according to the aforementioned global features. Searching for the closest matches to a given query vector in a large database is time consuming if the vector is even moderately high dimensional. Various methods have been

proposed to speed up the nearest neighbor retrieval, including hashing and tree structures [22]. However, the complexity of these methods grows exponentially with increasing dimensionality[23]. Therefore, I have adopted the RSVM method [20],inspired by the approaches of Internet search engines, to rank

the candidate samples in the database. Given a query qk, k = 1, 2, . . . , n and a sample collection

D = {d1, d2, . . . ,dm}, the optimal retrieval system should return a ranking r∗k, k = 1, 2, . . . , n, that orders the samples in D according to their relevance to the query. In this paper, the query q and the sample d are the Γ-dimensional global features as described earlier. In our approach, if a sample diis ranked higher than dj in some ordering r, i.e., r(di) > r(dj),then (di, dj) ∈ r; otherwise, (di, dj) _∈ r. Consider the class of linear ranking functions where w is a Lighted vector that is adjusted by learning and φ(q, d) is a pair wise distance function describing the match between q and d and can be defined as φi(q, d) = |qi − di|, i =1, . . . , Γ.

IV. EXPERIMENTAL RESULTS

I used the 3-D palm-print acquisition device developed in[14] to establish a 3-D palm-print database containing 8000samples collected from 400 palms. The 3-

$$H_w = \frac{1}{\sqrt{n}}\left[X_1 - m_1 \cdot e_1^T, \ldots, X_k - m_k \cdot e_k^T\right] \qquad (7)$$

$$H_b = \frac{1}{\sqrt{n}}\left[\sqrt{n_1}(m_1 - m), \ldots, \sqrt{n_k}(m_k - m)\right] \qquad (8)$$

$$H_t = \frac{1}{\sqrt{n}}(X - m \cdot e^T) \qquad (9)$$

D palm-print samples Ire collected in two separated sessions, ten samples in each session. The average time interval between the two sessions is 1 month. The collection procedure required volunteers to put their palms naturally and without force on the device. The original

ISSN: 2278 – 1323

spatial resolution of the data was 768 × 576. After ROI extraction, the central part (400 × 400) was extracted and down sampled to 200 × 200 for feature extraction and recognition.

The database was divided into a training part (the first session of 4000 samples) and a testing part (the second session of4000 samples). As described in Section III, the dimension of the proposed global features is 1 + N + N ×M. To select the values of M and N, I carried out a series of verifications on
the training database where the class of the input palm print was known. Each of the 3-D samples was matched with the remaining samples in the training database. A successful match is where the two samples are from the same class.

V. CONCLUSION

This paper has proposed three global features for 3-D palm print images: MD, HCA, and RLL. These cannot be extracted from 2-D palm prints and are not correlated with local features, such as line and texture features. To make these global features efficient for use in coarse classification, I treat them as a
multidimensional vector and use OLDA to map it to a lo Ir dimensional space. I then improve the efficiency of 3-D palm print recognition using two proposed approaches, coarse-level matching and RSVM, both of which significantly reduce the penetration rate during retrieval. Our recognition experiments using an established 3-D palm-print database of 8000 samples show that the global features improve palm-print classification which greatly reduces search times.

REFERENCES

[1] R. M. Bolle, J. H. Connell, S. Pankanti, N. K. Ratha, and A. W. Senior,Guide to Biometrics. New York: Springer-Verlag, 2003.
[2] A. W. K. Kong, D. Zhang, and G. M. Lu, "A study of identical 'twins' palm prints for personal verification," Pattern Recognition., vol. 39, no. 11,pp. 2149–2156, Apr. 2006.
[3] A. K. Jain and J. J. Feng, "Latent palm print matching," IEEE Trans. Pattern Anal. Mach. Intel., vol. 31, no. 6, pp. 1032–1047,Jun. 2009.
[4] D. Zhang, A. W. K. Kong, J. You, and M. Wong, "On-line palm print identification," IEEE Trans. Pattern Anal. Mach. Intel., vol. 25, no. 9,pp. 1041–1050, Sep. 2003.
[5] A. W. K. Kong and D. Zhang, "Competitive coding scheme for palm print verification," in Proc. Int. Conf. Pattern Recognition., 2004, vol. 1,pp. 520–523.
[6] Z. N. Sun, T. N. Tan, Y. H. Wang, and S. Z. Li, "Ordinal palm print representation for personal identification," in Proc. IEEE Int. Conf. Comput.Vis. Pattern Recogn., 2005, pp. 279–284.
[7] X. Q.Wu, D. Zhang, and K. Q.Wang, "Palm line extraction and matching for personal authentication," IEEE Trans. Syst., Man, Cybern. A, Syst.,Humans, vol. 36, no. 5, pp. 978–987, Sep. 2006.
[8] D. S. Huang, W. Jia, and D. Zhang, "Palm print verification based on principal lines," Pattern Recognit., vol. 41, no. 4, pp. 1316–1328,Apr. 2008.
[9] C. Samir, A. Srivastava, and M. Daoudi, "Three-dimensional face recognition using shapes of facial curves," IEEE Trans. Pattern Anal. Mach.Intel., vol. 28, no. 11, pp. 1858–1863, Nov. 2006.
[10] G. Medioni, J. Choi, C. H. Kuo, and D. Fidaleo, "Identifying non cooperative subjects at a distance using face images and inferred three dimensional face models," IEEE Trans. Syst., Man, Cybern. A, Syst.,
Humans, vol. 39, no. 1, pp. 12–24, Jan. 2009.
[11] P. Yan and K. W. Bowyer, "Biometric recognition using 3D ear shape,"IEEE Trans. Pattern Anal. Mach. Intel., vol. 29, no. 8, pp. 1297–1308,Aug. 2007.
[12] V. Srinivassan and H. C. Liu, "Automated phase measuring profilometry of 3D diffuse object," Appl. Opt., vol. 23, no. 18, pp. 3105–3108,Sep. 1984.
[13] H. O. Saldner and J. M. Huntley, "Temporal phase unwrapping: Application to surface profiling of discontinuous objects," Appl. Opt., vol. 36,no. 13, pp. 2770–2775, May 1997.
[14] D. Zhang, G. Lu, W. Li, L. Zhang, and N. Luo, "Palm print recognition using 3-D information," IEEE Trans. Syst., Man, Cybern. C, Appl. Rev.,vol. 39, no. 5, pp. 505–519, Sep. 2009.
[15] W. Li, D. Zhang, G. M. Lu, and N. Luo, "A novel 3-D palm print acquisition system," IEEE Trans. Syst., Man, Cybern. A, Syst., Humans, vol. 42,no. 2, pp. 443–452, Mar. 2012.

ISSN: 2278 – 1323